OPEN ACCESS
IOP PUBLISHING ENVIRONMENTAL RESEARCH LETTERS
Environ. Res. Lett. **8** (2013) 034032 (12pp) doi:10.1088/1748-9326/8/3/034032

Asynchronous exposure to global warming: freshwater resources and terrestrial ecosystems

Dieter Gerten[1], Wolfgang Lucht[1,2], Sebastian Ostberg[1], Jens Heinke[1,3], Martin Kowarsch[4], Holger Kreft[5], Zbigniew W Kundzewicz[1,6], Johann Rastgooy[1], Rachel Warren[7] and Hans Joachim Schellnhuber[1]

[1] Potsdam Institute for Climate Impact Research (PIK), Telegraphenberg, D-14473 Potsdam, Germany
[2] Department of Geography, Humboldt-Universität zu Berlin, Unter den Linden 6, D-10099 Berlin, Germany
[3] International Livestock Research Institute (ILRI), PO Box 30709, Nairobi 00100, Kenya
[4] Mercator Research Institute on Global Commons and Climate Change, Torgauer Straße 12–15, D-10829 Berlin, Germany
[5] Biodiversity, Macroecology and Conservation Biogeography Group, University of Göttingen, Büsgenweg 1, D-37077 Göttingen, Germany
[6] Polish Academy of Sciences, Institute for Agricultural and Forest Environment, ulica Bukowska 19, 60809 Poznań, Poland
[7] Tyndall Centre, School of Environmental Sciences, University of East Anglia (UEA), Norwich NR4 7TJ, UK

E-mail: gerten@pik-potsdam.de

Received 3 May 2013
Accepted for publication 28 August 2013
Published 12 September 2013
Online at stacks.iop.org/ERL/8/034032

Abstract
This modelling study demonstrates at what level of global mean temperature rise (ΔT_g) regions will be exposed to significant decreases of freshwater availability and changes to terrestrial ecosystems. Projections are based on a new, consistent set of 152 climate scenarios (eight ΔT_g trajectories reaching 1.5–5 °C above pre-industrial levels by 2100, each scaled with spatial patterns from 19 general circulation models). The results suggest that already at a ΔT_g of 2 °C and mainly in the subtropics, higher water scarcity would occur in >50% out of the 19 climate scenarios. Substantial biogeochemical and vegetation structural changes would also occur at 2 °C, but mainly in subpolar and semiarid ecosystems. Other regions would be affected at higher ΔT_g levels, with lower intensity or with lower confidence. In total, mean global warming levels of 2 °C, 3.5 °C and 5 °C are simulated to expose an additional 8%, 11% and 13% of the world population to new or aggravated water scarcity, respectively, with >50% confidence (while ~1.3 billion people already live in water-scarce regions). Concurrently, substantial habitat transformations would occur in biogeographic regions that contain 1% (in zones affected at 2 °C), 10% (3.5 °C) and 74% (5 °C) of present endemism-weighted vascular plant species, respectively. The results suggest nonlinear growth of impacts along with ΔT_g and highlight regional disparities in impact magnitudes and critical ΔT_g levels.

Keywords: climate change impacts, water scarcity, water resources, terrestrial ecosystems, impact functions

S Online supplementary data available from stacks.iop.org/ERL/8/034032/mmedia

1. Introduction

Countries' current pledges to reduce greenhouse gas emissions would set global mean temperature increase (ΔT_g) on a trajectory of ~3.5 °C above pre-industrial levels by the end of this century (Rogelj *et al* 2010)—far above the 2 °C target adopted in the Cancún Agreements (UNFCCC 2011). The tensions about the climate policy goal of limiting ΔT_g to 2 °C require that policymakers be informed about possible consequences of their decisions. This can be accomplished by solid scientific assessments of the presumably high costs, the implementation risks and the benefits (in terms of avoided climate change impacts) of low-stabilization targets on the one hand and of consequences of less ambitious mitigation (i.e. global warming above 2 °C) on the other hand (Knopf *et al* 2012). To contribute to a better understanding of the latter, this study quantifies—spatially explicitly at global scale—how freshwater availability and terrestrial ecosystems might change in response to different levels of ΔT_g.

Previous assessments of (exposure to) impacts associated with different ΔT_g levels were compromised by a number of methodological inconsistencies, as pointed out e.g. by Lenton (2011) and Warren *et al* (2011). 'Reasons for concern' (Smith *et al* 2009) and 'burning ember' diagrams (Schneider and Mastrandrea 2005) often combine heterogeneous, partly qualitative impact estimates that lack spatial and temporal detail and do not systematically account for available climate change scenarios. Simulation models or other internally consistent balancing schemes, applied for the whole land surface and forced by simulations from a large ensemble of general circulation models (GCMs), can in principle overcome these inconsistencies. However, respective studies either focused on single, though politically relevant ΔT_g levels (Fung *et al* 2010, Zelazowski *et al* 2011) or could not consider the structural uncertainty among GCMs—which is sizeable due to the large spread especially in precipitation projections (e.g. Knutti and Sedláček 2012). Often projections from only a few GCMs were used (Arnell *et al* 2011) or ensemble projections were grouped according to the warming level reached by the end of this century (Scholze *et al* 2006), which strongly reduces the sample size for higher ΔT_g levels due to differences in the GCMs' climate sensitivity (see Rogelj *et al* 2012). Other studies (Tang and Lettenmaier 2012) selected those future time periods when a given ΔT_g value was exceeded, which means that the timing of the T_g changes differed among GCMs. Yet other studies only investigated when and where specific temperatures or warming rates are likely to be reached, without quantifying resulting impacts (Joshi *et al* 2011, Mahlstein *et al* 2013).

To overcome many of these problems, we here employ a newly generated ensemble of 152 climate scenarios (Heinke *et al* 2012), constructed by performing a 'pattern-scaling' of stylized ΔT_g trajectories (reaching 1.5–5 °C above pre-industrial levels around year 2100, in 0.5° steps) with 19 GCMs from the CMIP3 archive. Used as forcing for the well-validated LPJmL biosphere and water balance model (Sitch *et al* 2003, Gerten *et al* 2004, Bondeau *et al* 2007), this setup enables consistent quantification of impacts for different ΔT_g levels and underlying climate policies, respectively. The local–global scaling factors are nearly independent of the considered emissions scenarios and are sufficiently accurate over a wide range of ΔT_g, especially in case of temperature but less so in case of precipitation (Mitchell 2003; see Heinke *et al* 2012 for details on this approach).

We present our results acknowledging that climate change proceeds asynchronously across the globe (i.e. some regions are affected earlier by significant changes than others; Joshi *et al* 2011, Mahlstein *et al* 2011) and that regions differ with respect to their vulnerability to such change (Füssel 2010). In so doing, we highlight which regions are likely to experience the here considered critical changes to water availability and ecosystems 'earlier' (i.e. at lower ΔT_g levels around 2100) than others. To communicate these spatiotemporal patterns of exposure—and of implied global inequalities—we directly map the ΔT_g level at which the local impacts on water and ecosystems first occur. We also demonstrate the incremental changes between different ΔT_g levels.

2. Methods

2.1. Climate scenarios

We rearranged pre-existing GCM simulations using a pattern-scaling approach to allow for analysis of impacts under different levels of ΔT_g while accounting for differences among GCMs. The principle of pattern-scaling is to calculate scaling coefficients that statistically link local changes in climate variables to ΔT_g, global fields of which can be used in spatially resolved impact models.

The scaling coefficients were derived for each calendar month, for each grid cell over land (0.5° × 0.5° spatial resolution), and for each of 19 GCMs that participated in the World Climate Research Programme's Coupled Model Intercomparison Project (CMIP3) (Meehl *et al* 2007) to account for the large differences in GCM projections (see e.g. Knutti *et al* 2010). For each GCM and month, this procedure yielded the local change in climate variables (air temperature, precipitation amount, degree of cloudiness) per degree of ΔT_g. These response patterns were then combined with time series of annual ΔT_g derived from the reduced-complexity climate model MAGICC6 (Meinshausen *et al* 2011). Greenhouse gas emissions were tuned in MAGICC6 in a way that ΔT_g levels of 1.5, 2.0, 2.5, 3.0, 3.5, 4.0, 4.5 and 5 °C above pre-industrial levels (from the GCMs' unforced control runs) are reached by around year 2100 (2086–2115 average). Corresponding atmospheric CO_2 concentrations range between ~400 ppm (for the 1.5 °C trajectory) and ~1400 ppm (for the 5 °C trajectory). As a result of this data fusion, 19 climate change patterns were obtained for each ΔT_g step—152 scenarios altogether. The patterns were applied as anomalies to 1980–2009 observed climate (CRU TS3.1 for temperature and cloudiness, Mitchell and Jones 2005; and GPCC dataset versus 5 for precipitation, Rudolf *et al* 2010), yielding the 152 monthly time series up to year 2115. These data were subsequently interpolated to

daily values using stochastic procedures as in Gerten *et al* (2004) and then used to force the LPJmL model for assessing potential impacts (see following sections). A comprehensive description of the generation of the scaling patterns and of the anomaly approach is provided by Heinke *et al* (2012). While biases in GCM projections have been accounted for in this data processing, we recognize that the skill of GCMs to project climate changes at regional scale is limited, as has been shown in a number of studies for CMIP3 models (e.g. Pincus *et al* 2008, Hawkins and Sutton 2010). Thus, the present scenarios are suited to identify the broad patterns of climate changes and their impacts (presented in global- and continental-scale plots and tables), but results for individual grid cells (presented in maps) should be interpreted with caution.

2.2. The LPJmL model

For quantifying the below-specified changes to water availability and ecosystems for each climate scenario, we employed the process-based LPJmL dynamic global vegetation and water balance model (Sitch *et al* 2003, Gerten *et al* 2004; with recent overall improvements by Bondeau *et al* 2007 and Rost *et al* 2008 but with crop, irrigation and river routing modules switched off—see section 2.3.1). LPJmL computes the growth and productivity of the world's major vegetation types (here, nine plant functional types) in direct coupling with associated fluxes of water and carbon in the vegetation–soil system. The model was run at daily time step and 0.5° × 0.5° spatial resolution globally, forced by the pattern-scaled time series of daily climate (air temperature, precipitation amount, number of wet days per month, cloud cover) and yearly atmospheric CO_2 concentration. The model has been shown to well reproduce observed vegetation distribution, biomass production and carbon fluxes (Lucht *et al* 2002, Sitch *et al* 2003, Hickler *et al* 2006, Bondeau *et al* 2007), fire regimes (Thonicke *et al* 2001) and water fluxes (Gerten *et al* 2004, Rost *et al* 2008, Fader *et al* 2010). Hence, although individual process representations require continuous improvement in this model and others of its type (e.g. Sitch *et al* 2008, Li *et al* 2012, Murray *et al* 2013, Piao *et al* 2013), LPJmL is a suited tool for assessing climate change effects on water resources and ecosystems alike.

2.3. Change metrics

We consider local changes in water availability/scarcity and terrestrial ecosystems as expressed by two metrics, and subsequently relate these changes to the *in situ* human population size and 'species endemism' of vascular plants, respectively (see following paragraphs). The metrics are calculated for each 0.5° grid cell, ΔT_g step and GCM pattern. The global warming level deemed critical from a local perspective is given by the lowest ΔT_g value at which the metrics cross specific thresholds in the 2086–2115 average. We focus on changes projected to be 'more likely than not' (found in >50%, i.e. at least 10 out of the 19 climate change scenarios) but also address 'likely' (>66%) and 'unlikely' (<33% but >0%) impacts, following IPCC guidance notes (Mastrandrea *et al* 2010). We also focus on three policy-relevant ΔT_g levels: the 2 °C mitigation target; the likely outcome of current national emissions reduction pledges (3.5 °C); and a business-as-usual case (5 °C, near to the average ΔT_g simulated by GCMs under high-emission SRES A1FI and RCP8.5 scenarios; Rogelj *et al* 2012). Since there are interdependencies among GCMs (Masson and Knutti 2011, Pennell and Reichler 2011), actual confidence may be narrower than stated herein. Moreover, although we have integrated all GCM runs with different initial conditions available from the CMIP3 archive (see Heinke *et al* 2012), they embody only a fraction of possible climate developments in the future (Rowlands *et al* 2012).

2.3.1. Water scarcity. Chronic supply-side water scarcity—likely to increase competition among water users and to constrain food production, economic development and environmental integrity—is defined to prevail if <1000 m^3 cap^{-1} yr^{-1} are available within a given spatial unit (Falkenmark and Widstrand 1992). This analysis uses river basins as the spatial unit, delineated as in Haddeland *et al* (2011), which implicitly assumes that any water demand is to be met within each basin, neglecting e.g. import of water-intensive products from other regions (Fader *et al* 2011). Furthermore, we consider only 'blue' water resources, i.e. renewable surface and subsurface runoff useable for irrigation, industries and households. Applying more complex water scarcity indicators and of other mapping units may yield different results (Gerten *et al* 2011). Runoff was computed under conditions of potential natural vegetation, for reasons of consistency with the assessment for ecosystems; irrigation, reservoir operation and land use change effects are thus not considered in this study. We distinguish four types of change to water resources and scarcity.

(1) *Regions already chronically water-scarce experience aggravated scarcity.* This is the case if the simulated annual and/or monthly runoff is significantly lower in the future (2086–2115 period) than presently (1980–2009). A significant decrease in the average annual runoff is assumed if its change is greater than present standard deviation (Gosling *et al* 2010, Arnell *et al* 2011), which can be regarded as a challenge to water management systems attuned to historic flow experience. A significant decrease in monthly runoff—taken as a proxy for increased drought frequency on top of the change in mean annual flow (Lehner *et al* 2006)—is assumed if the median of calendar months in the future is lower than the respective present-time median in more than 10% (i.e. 36) of the future months.

(2) *Regions not yet chronically water-scarce move into a water-scarce status*—i.e. <1000 m^3 cap^{-1} yr^{-1} are simulated to be available in the future in regions that are above this threshold today.

(3) *Regions not chronically water-scarce experience lower water availability*. In this case the decrease in water availability is defined as in (1), yet applied to regions with >1000 m^3 cap^{-1} yr^{-1} both presently and in the future.

(4) *Regions that are water-scarce but do not experience aggravated scarcity*; i.e. regions where present water availability is <1000 m^3 cap^{-1} yr^{-1} but does not cross the thresholds cf case (1). Human populations are either held constant at year 2000 values or assumed to change according to the SRES B1 or A2r population projections, respectively (Grübler *et al* 2007). Increases in runoff are also analysed, but for reasons of brevity we do not relate them to the number of people living in areas affected by such increases.

2.3.2. Ecosystem change. Severe ecosystem changes are assumed if the change in a generic ecosystem stability index 'Γ' developed by Heyder *et al* (2011) adopts a value ≥ 0.3 (moderate changes, $\Gamma > 0.1$). This can be interpreted as simultaneous shifts in several ecosystem features as large as those associated with e.g. a transition from temperate forest to boreal forest. The Γ metric is composed of a suite of biogeochemical and vegetation structural variables, changes in which either represent alterations in the entire ecosystem status or in a specific subset of variables. Using such an aggregated index advances earlier studies focused solely on biome area changes (Leemans and Eickhout 2004) or individual ecosystem properties (Gerber *et al* 2004, Scholze *et al* 2006, Sitch *et al* 2008).

Specifically, Γ encompasses the following components: (1) *carbon fluxes* (net primary production, heterotrophic soil respiration, carbon release from natural fires), (2) *water fluxes* (runoff, evaporation, transpiration), (3) *carbon stocks* (in plants and soils), and (4) *vegetation composition* ('ΔV' metric measuring structural dissimilarity of ecosystems based on life forms (trees, grass, bare ground) and their leaf architecture and phenology (needle-leaved or broadleaved, evergreen or deciduous; Sykes *et al* 1999)). Γ combines relative and absolute changes in these variables as well as changes in the proportional relation of carbon and water fluxes to each other. Some components are also scaled according to their signal-to-noise ratio. The overall Γ metric is finally normalized to values between 0.0 meaning no change and 1.0 meaning total restructuring of the considered basic ecosystem features. It was calculated for the uncultivated fraction of grid cells, thus maps and aggregated global values refer to the respective fractions of grid cells only. For a complete description of Γ see Heyder *et al* (2011), and also Ostberg *et al* (2013) who analyse it in more detail for the same climate scenarios as used here.

While Γ can be interpreted as overall habitat changes, the simulations do not contain information at species level. To frame the model results in the context of floral biodiversity (rather than merely counting the total area affected by $\Gamma > 0.3$ or >0.1 as in Ostberg *et al* 2013), we linked them to an independent global dataset of vascular plant (ferns, gymnosperms, angiosperms) biodiversity (Kier *et al* 2009). The dataset contains information on the current fractional distribution, species richness and endemism for each of 90 unique terrestrial (island and mainland) biogeographic regions—315 903 species altogether. The here used 'endemism richness' is the weighted product of the number of species within a biogeographic region and the region's share (0–1) of each species' global distribution range. For example, if 20% of a species' distribution range falls into a region, 20% of the total species number is attributed to it.

We determined, for each ΔT_g step, which biogeographic regions experience changes in Γ on more than a third of their respective area, and counted how many of the 19 climate scenarios show this. We then determined the endemism richness of each of those regions from the Kier *et al* (2009) dataset, and aggregated the values to continental and global sums. Note that endemism richness refers to the present situation, whilst climatic and land cover changes may concurrently alter species richness and endemism (Sommer *et al* 2010). That is, our results do not indicate the climate effects on future endemism richness; they rather indicate the changing biogeochemical boundary conditions.

3. Results

3.1. Aggravation or new establishment of water scarcity

Figure 1 illustrates that certain regions are affected by the here assessed changes at low ΔT_g levels already, under $>50\%$ of the climate change patterns, whereas others are affected not before higher ΔT_g levels are reached. People inhabiting river basins particularly in the Middle East and Near East become newly exposed to chronic water scarcity or experience an aggravation of existing scarcity even if highly ambitious mitigation policies could constrain ΔT_g to $\leq 2\,^\circ$C (figure 1(a)). For these regions, GCMs project significantly lower rainfall even in low-emission scenarios (Bates *et al* 2008), resulting in less runoff (figure 2(a)). Of the $\sim$1.3 billion contemporary population exposed to water scarcity (table 1), 3% (North America) to 9% (Europe) are prone to aggravated scarcity at $\Delta T_g \leq 2\,^\circ$C. An additional 0–2% of each continent's population live in basins simulated to become water-scarce (figure 3(a), top panel). In total, 486 million people—about 8% of the world population in 2000 (equalling almost that year's population of the US and Indonesia together)—are affected by either of these changes at $\Delta T_g \leq 2\,^\circ$C.

Conversely, more runoff is simulated especially for high latitudes and parts of the tropics at $\Delta T_g > 3.5\,^\circ$C (figure 2(b)). Associated shifts in seasonal hydrographs and higher flood risk compared to historical experience cannot be ruled out for those regions (Kundzewicz *et al* 2008), but this is not investigated in detail here as we focus on regions with decreases in runoff.

Many of the regions not significantly affected at $\Delta T_g \leq 2\,^\circ$C are projected to become (more) water-scarce if T_g increased by up to $3.5\,^\circ$C—a scenario that cannot be dismissed, if no further commitments were made than current emissions reduction pledges. This concerns e.g. the Middle East, North Africa and South Europe (figure 1(a)), i.e. regions inhabited by another 3% of the world population (adding to the 8% increase at $2\,^\circ$C; see figure 4(a)). At $\Delta T_g > 3.5\,^\circ$C, the climate change effects expand further into these regions, such that 12–15% of each continent's population (Australasia, 23%) and 13% of the world population are exposed to aggravated or newly established water scarcity at $\Delta T_g = 5\,^\circ$C under $>50\%$ of the climate patterns (figure 3(a)).

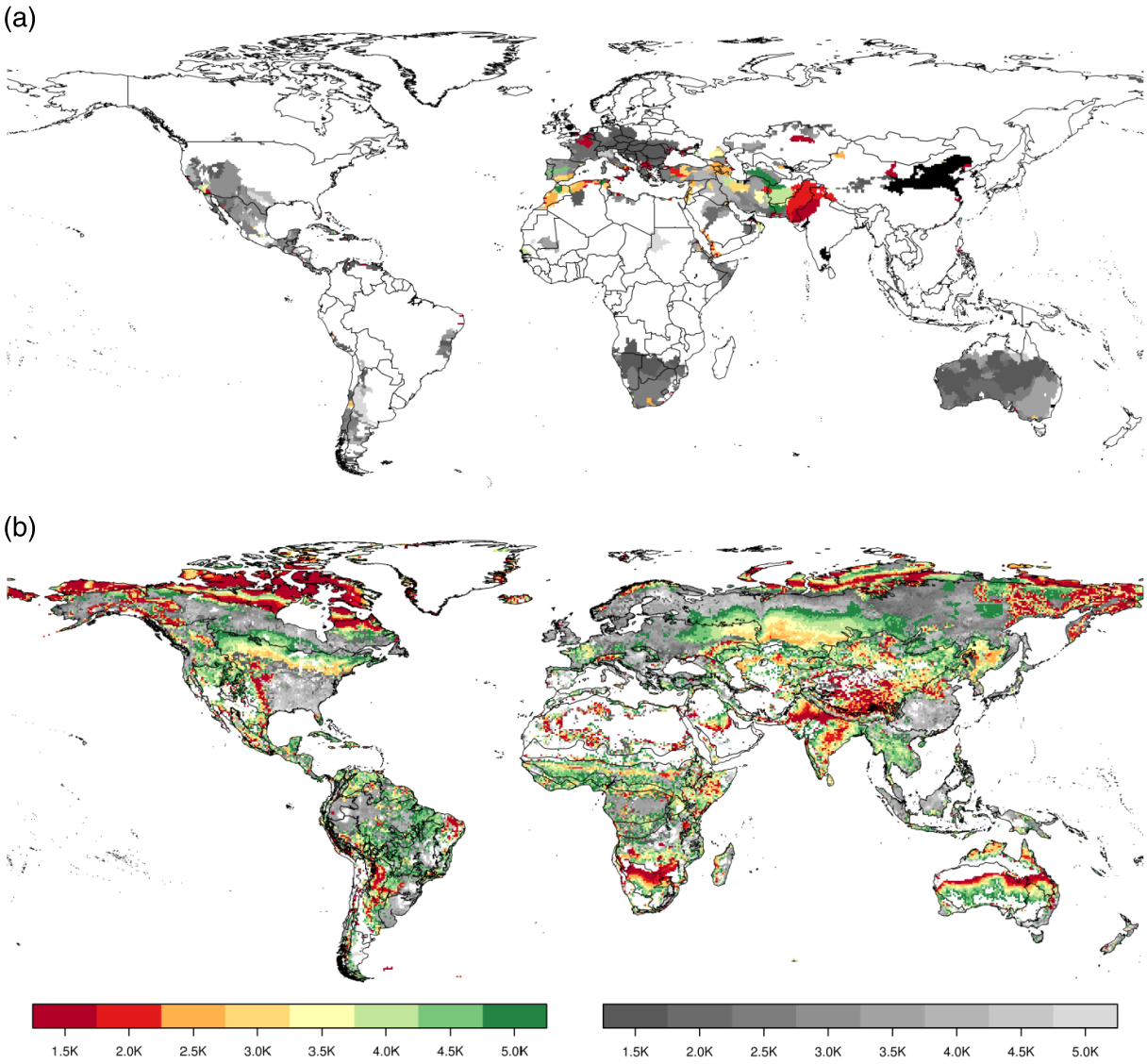

Figure 1. Threshold level of ΔT_g leading to significant local changes in water resources (a) and terrestrial ecosystems (b). (a) Coloured areas: river basins with new water scarcity or aggravation of existing scarcity (cases (1) and (2), see section 2.3.1); greyish areas: basins experiencing lower water availability but remaining above scarcity levels (case (3)); black areas: basins remaining water-scarce but without significant aggravation of scarcity even at $\Delta T_g = 5\,^{\circ}\mathrm{C}$ (case (4)). No population change is assumed here (see figure S5 available at stacks.iop.org/ERL/8/034032/mmediafor maps including population scenarios). Basins with an average runoff <10 mm yr^{-1} per grid cell are masked out. (b) Regions with severe (coloured) or moderate (greyish) ecosystem transformation; delineation refers to the 90 biogeographic regions. All values denote changes found in $>50\%$ of the simulations.

This increase is attributable primarily to Asia (see figure 3(a) bottom panel), while contributions from other continents are comparatively minor. Given the SRES B1 and A2r demographic projections, a higher fraction of the future world population would be exposed to water scarcity than around year 2000, i.e. 30–43% (∼2–5 billion cf table 1; also see figure S5 available at stacks.iop.org/ERL/8/034032/mmedia). Note that the relative increase in the number of people exposed to new or aggravated water scarcity due to climate change only is largely independent of the population scenario, as was also found by Gosling *et al* (2010).

3.2. Severe changes to terrestrial ecosystems

Substantial biogeochemical and vegetation structural shifts in terrestrial ecosystems are simulated under more than half of the climate patterns for a mean global warming of 2 °C (figures 1(b) and 3). In particular, this concerns high latitudes (reflecting higher primary production and northward migration of the treeline), and also semiarid regions on all continents (reflecting CO_2-induced improvements in plant water use efficiency and expanding vegetation cover) (Heyder *et al* 2011). These areas represent 11% of the ice-free, unmanaged global land surface (details in Ostberg *et al* 2013). But, due to the highly uneven distribution of species richness around the world, they represent only 4—albeit spatially quite extensive—unique biogeographic regions that altogether entail 1% of global endemism richness of vascular plants (table 1, figure 4(b)). The number of biogeographic regions exposed to severe habitat changes is found to quadruple at $\Delta T_g = 3.5\,^{\circ}\mathrm{C}$, then affecting 10% of

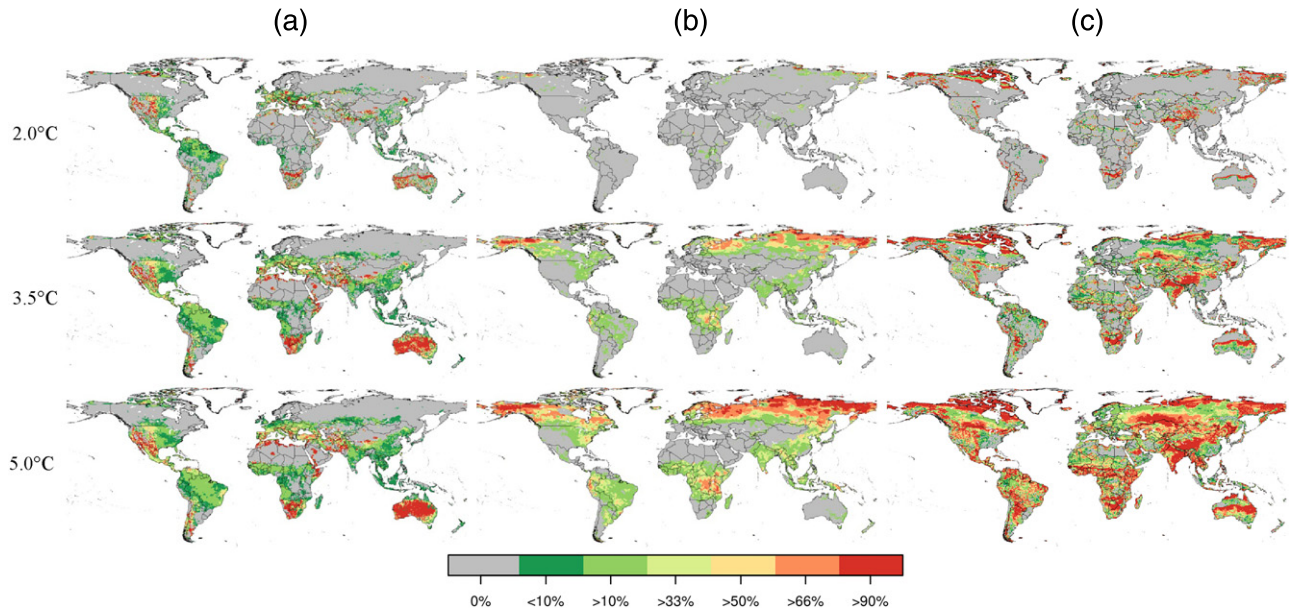

Figure 2. Likelihood of a decrease in runoff (a), an increase in runoff (b) and a severe change in ecosystems (c) for selected ΔT_g levels. (a) and (b) show whether the simulated decrease (increase) in average annual runoff exceeds present (1980–2009) standard deviation, or whether monthly runoff is >10% more frequently below (above) its present median. Areas with presently <10 mm yr^{-1} are masked out. The likelihoods are derived from the 19 climate change patterns. See figures S1–S4 (available at stacks.iop.org/ERL/8/034032/mmedia) in the supplement for all eight ΔT_g levels.

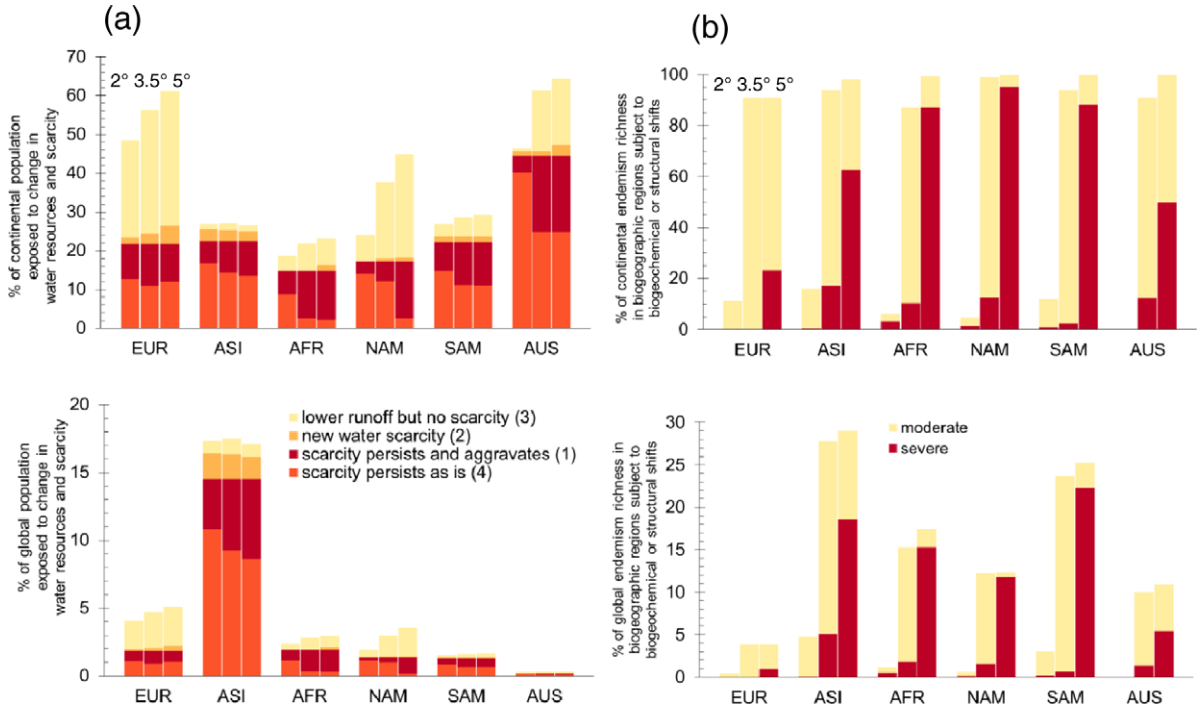

Figure 3. Continental-scale effects of selected ΔT_g levels (2 °C, left bars; 3.5 °C, middle bars; 5 °C, right bars), simulated under >50% of the climate change patterns. (a) Percentage of continental population exposed to new or aggravated water scarcity, or lower water availability outside water-scarce river basins, assuming unchanged population. (b) Percentage of continental endemism-weighted species richness of vascular plants in biogeographic regions exposed to substantial habitat shifts ($\Gamma > 0.3$ on >33% of the regions' area). The upper panel shows values relative to the continental totals, whereas the bottom panel shows values relative to the global totals. Numbers in brackets refer to the four cases of hydrologic change (see section 2 and figure 1). EUR, Europe; ASI, Asia; AFR, Africa; NAM, North America; SAM, South America; AUS, Australasia.

endemism richness. The incremental exposure steeply rises further if warming continued above this level: our simulations suggest that 68 out of the 90 distinct biogeographic regions—presently containing $\sim\frac{3}{4}$ of today's vascular plant endemism richness—would be subject to pronounced habitat transformation at 5 °C (figure 4(b)). Even higher shares

Table 1. Continental and global effects of different ΔT_g levels. Top: millions of people living in river basins characterized by chronic water scarcity (<1000 m^3 cap^{-1} yr^{-1}) (cases (2) and (4)), either with or without B1 and A2r future population change. People in water-scarce basins that show an aggravation of scarcity according to case (1) (see figure 3(a)) are not counted here. Numbers in brackets denote the changes (relative to the present) that are solely due to climate change. Bottom: number of unique biogeographic regions (out of 90) exposed to severe biogeochemical or vegetation structural shifts. All values refer to changes with >50% confidence, simulated under at least 10 of the 19 GCM patterns.

			Climate change only			Climate and B1 population change				Climate and A2r population change			
	Around 2000		Affected				Affected				Affected		
	Total	Affected	+2.0 °C	+3.5 °C	+5.0 °C	Total	+2.0 °C	+3.5 °C	+5.0 °C	Total	+2.0 °C	+3.5 °C	+5.0 °C
	People living in water-scarce basins												
Europe	505	110	118	123	133	465	143	145	133	531	258	237	186
Asia	3879	870	988	985	970	3733	1424	1480	1442	6 929	3463	3440	3401
Africa	775	115	115	115	126	1647	313	304	295	3 145	1084	925	867
N America	479	83	81	86	87	712	137	121	127	891	270	274	259
S America	345	77	82	82	82	407	87	89	89	747	198	167	165
Oceania	29	13	13	13	14	44	16	18	18	55	19	20	20
Globe	6012	1267	1397 (+130)	1404 (+137)	1412 (+145)	7009	2120 (+628)	2157 (+665)	2103 (+611)	12 298	5294 (+293)	5063 (+62)	4897 (−104)
	Number of unique biogeographic regions with severe ecosystem changes on >33% of their area												
Europe	3	—	—	—	2								
Asia	22	—	1	6	16								
Africa	18	—	1	4	13								
N America	10	—	1	2	10								
S America	26	—	1	3	21								
Oceania	10	—	—	1	6								
Globe	90	—	4	16	68								

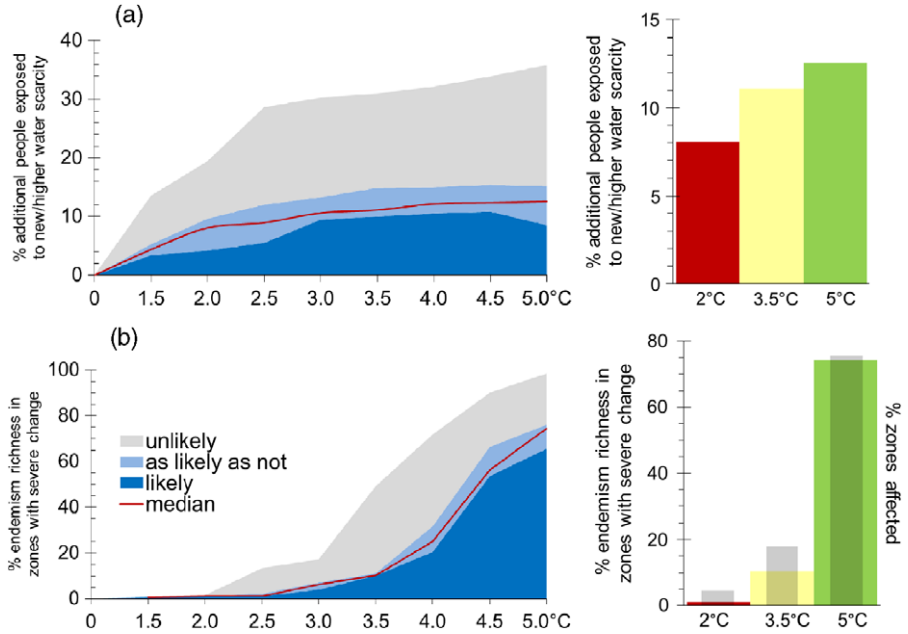

Figure 4. Simulated exposure of world population to water scarcity (a) and of global endemism richness to severe habitat changes (b), plotted as functions of ΔT_g. Left panel: function for all $8\Delta T_g$ levels and three confidence levels (stacked plot); right panel: results highlighted for 2, 3.5 and 5 °C and the >50% case. Specifically, (a) shows the additional percentage of current world population exposed to new or aggravated water scarcity (cases (1) and (2); see section 2.3.1); (b) shows the percentage of global vascular plant endemism richness presently residing in regions that will be exposed to substantial habitat shifts (>33% of a region's area with $\Gamma > 0.3$). Grey bars in (b) show the corresponding number of affected regions (% out of the 90 regions; plotted on the same axis).

of continental endemism richness are reached in Africa and the Americas at 5 °C (figure 3(b), top panel). Severe ecosystem changes on these two continents are simulated for regions presently containing half of the world's vascular plant endemism richness (see figure 3(b), bottom panel). Results tend to concur with regional studies that suggest significant declines in floral and faunal species richness at ΔT_g above ~3 °C (Hare *et al* 2011).

3.3. Moderate or less confident changes

When choosing lower 'critical' thresholds (including non-water-scarce basins and, respectively, areas with $0.1 < \Gamma < 0.3$) or considering changes simulated under less than 50% of the climate patterns, exposure to change generally occurs at lower ΔT_g and covers larger areas. This is indicated by the following examples (figures compiled in the supplement available at stacks.iop.org/ERL/8/034032/mmedia). The incremental impact on ecosystems between 2 and 3.5 °C is significantly stronger when accounting for moderate ecosystem changes in addition to severe ones, in terms of both the size of the affected area (figure S6(d) available at stacks.iop.org/ERL/8/034032/mmedia) and the number and endemism richness of the underlying biogeographic regions (figure S7 available at stacks.iop.org/ERL/8/034032/mmedia). If reductions in water availability are computed also for non-water-scarce basins in addition to the reductions in water-scarce regions, many regions especially in Europe, Australia and southern Africa appear to be affected already at 1.5 °C (figure S6(a)). For a 5 °C warming, this would mean that ~20% of the world population is exposed to some form of significantly reduced water availability (figure S7). Finally, inclusion of unlikely changes (<33% of the simulations) suggests a substantially larger globally affected population (water scarcity) and area (ecosystem change) compared to the >50% case, for all ΔT_g levels (figure S6). Note that 'unlikely' here represents changes that cannot be ruled out scientifically, as they occur under simulations from at least one of the 19 GCMs—each of which we here consider equally plausible.

4. Discussion

Albeit confined to selected change metrics, the present assessment accentuates asynchronies in exposure to climate change. That is, different regions are exposed to hydrologic or ecosystem changes at different ΔT_g levels, as displayed in figure 1. Moreover, the study suggests that global and continental impacts accrue—in part nonlinearly—with ΔT_g and that the shape of this growth curve differs between impact sectors.

For ecosystems, the climate response functions tend to display a sigmoidal shape with a slow initial increase, a rapid expansion in a critical range at intermediate ΔT_g levels, and a plateau at high ΔT_g when changes cover most regions (figure 4(b); note that the shape hardly depends on the confidence level, i.e. the number of climate scenarios). Regarding the additional population in water-scarce regions, the curve is much flatter, i.e. the incremental global effect of high ΔT_g levels is weaker. It can also be noted, for

Asia, that the population exposed to water scarcity slightly decreases at high ΔT_g (table 1, representing case (2) category in figure 3(a) and possibly also basins that move out of the water-scarce category). This is probably due to nonlinearities in the relationship between forcing and hydrological response in a few, densely populated regions where e.g. effects of higher precipitation at high ΔT_g may outdo effects of higher evapotranspiration. Detailed explanation of such developments would require model runs in which different driving forces are held constant. In general, different shapes of impact functions are found for change metrics other than those studied here, and also for individual regions (compare e.g. Levermann *et al* 2012, Schaphoff *et al* 2013).

Expert judgements suggest that abrupt, potentially irreversible biospheric 'tipping points' may be reached if ΔT_g exceeds a critical range (Amazonian forest decline, +3–4 °C; boreal forest decline, +3–5 °C; Lenton *et al* 2008). While such events are not studied here, our results partly support these concerns. As shown in figure 1(b), widespread ecosystem changes and implied forest die-back in the southern boreal zone and some other regions are simulated under >50% of the climate patterns if ΔT_g exceeded ~3.5 °C, due primarily to heat stress and also droughts (as is already evident in some regions; Allen *et al* 2010). However, large-scale change to Amazonian ecosystems—characterized by high endemism richness—is simulated only for ΔT_g levels close to the maximum range considered here, i.e. 5 °C (figure 2(c)). Recent findings also suggest that Amazonian die-back is found under a few climate change scenarios only, and that the (highly uncertain) CO_2 effects on vegetation play a major role (Rammig *et al* 2010, Huntingford *et al* 2013). The simulated system transition in savannah-dominated regions agrees with recent evidence for local regime shifts (Higgins and Scheiter 2012), with C4 grass benefitting from low ΔT_g and woody encroachment benefitting directly from the elevated CO_2 concentration associated with higher ΔT_g. Furthermore, in the boreal zone, permafrost thawing (not considered in the present model setup) will, due to higher microbial activity, augment soil carbon release even further than implied in our simulations, probably producing a positive feedback to warming (Schneider von Deimling *et al* 2012, Schaphoff *et al* 2013).

The here used climate change scenarios were constructed so that different ΔT_g levels are reached around year 2100. In current high-emission scenarios, however, the prospective timing of $\Delta T_g = 2$ °C is around 2050 and that of $\Delta T_g = 3.5$ °C around 2080 (Rogelj *et al* 2012). Hence, in case such scenarios will come true, the demonstrated changes in water scarcity and Γ would occur some decades earlier than assumed herein. A related caveat, which merits quantification in further studies, is that the timing of ΔT_g and associated local climate changes could be of importance. This is particularly true for ecosystems, whose adaptation capacities may be weaker or whose response to climate change may be slower than assumed in our model (Loarie *et al* 2009, Sandel *et al* 2011, Diffenbaugh and Field 2013). There is also scope to investigate how much of the difference in impacts between ΔT_g levels is due only to the corresponding differences in atmospheric CO_2 concentration. In fact, besides the radiative (climate) effects of CO_2, there are direct physiological and structural effects on plants, with implications for both water scarcity and Γ. These effects are accounted for in the LPJmL model (Leipprand and Gerten 2006), but different assumptions about the relationship between CO_2 and ΔT_g (e.g. due to other emissions trajectories and climate sensitivities) may produce somewhat different responses. Furthermore, not only GCMs but also impact models (including vegetation models such as the one used here) differ in terms of model structure and parameterization, thus introducing a further level of uncertainty. Resulting uncertainties regarding the Γ metric and variants of the hydrologic metric used herein have been analysed recently (Piontek *et al* 2013, Schewe *et al* 2013).

5. Conclusions

Our comprehensive simulations show that both freshwater availability and ecosystem properties will change significantly in the future if no efforts were made to abate global warming. The impacts seem to accrue in nonlinear ways, though the shape of impact functions differs among the considered variables. Even if global warming was limited to 1.5–2 °C above pre-industrial level in accordance with current negotiations, almost 500 million people might be affected by an aggravation of existing water scarcity or be newly exposed to water scarcity. Concurrent population growth would further increase this number to up to around 5 billion people. This outlook is basically supported by findings from Schewe *et al* (2013) based on a large suite of global hydrological models. Strongest effects on terrestrial ecosystems appear to occur at somewhat higher global warming levels, with the sharpest increase in the affected area (and underlying plant biodiversity) beyond 3–3.5 °C. These global changes are simulated to be made up by a heterogeneous spatial pattern of change (which differs among impact variables), and different regions will be affected at different ΔT_g levels (as summarized in figure 1).

Besides their obvious relevance for the affected regions themselves, the complex patterns of exposure to climate change might be of political and ethical concern when considering global mitigation targets and related impacts. For example, they shed interesting light on the ethical responsibility of high-emission countries, which—if accepted—could have bearing on both mitigation and adaptation burden sharing (Srinivasan *et al* 2008). Furthermore, the present results inform, but also complicate decisions about a fair allocation of international adaptation funds to different regions today. Such aspects will have to be explored in future studies, possibly relating the patterns of exposure to patterns of emissions underlying the climate change scenarios.

We emphasize that the here simulated changes to terrestrial ecosystems cover vast areas, which poses the question whether these changes are manageable, especially under conditions of rapid change and continued anthropogenic landscape modifications (Millar *et al* 2007). Decreases

in water availability appear to be less widespread and may partly be buffered through adaptive management (not quantified here), even though climate change undermines the conventional assumption of stationary water resources (as reflected in our analysis of whether future changes exceed present variability; also see Milly *et al* 2008). At any rate, it is questionable whether adaptive water management will be sufficient to meet increasing water and food demands of a growing world population (Rost *et al* 2009). As a consequence, further expansion of irrigated or rainfed cropland may be needed, which would, in turn, amplify the climate change impact on Γ on those areas.

In sum, the present results plea for more comprehensive studies of whether critical ranges for a larger selection of impacts do cluster around a certain ΔT_g level (as suggested already by Parry *et al* 2001, Schellnhuber *et al* 2004). Ultimately, this requires multi-sectoral impact model intercomparisons in an interdisciplinary scientific community effort, now under way (Arnell *et al* 2013, Piontek *et al* 2013).

Acknowledgments

This research was supported by the 6th and 7th Framework Programmes of the European Communities under grant agreements no. 036946 (WATCH) and 265170 (ERMITAGE), the BMBF-funded project GLUES, and the CGIAR research program on Climate Change, Agriculture and Food Security. We thank Katja Frieler and Malte Meinshausen for preparing the MAGICC6 data, Sibyll Schaphoff and Werner von Bloh for technical support, and anonymous reviewers for constructive comments.

References

Allen C D *et al* 2010 A global overview of drought and heat-induced tree mortality reveals emerging climate change risks for forests *Forest Ecol. Manag.* **259** 660–84

Arnell N W, van Vuuren D P and Isaac M 2011 The implications of climate policy for the impacts of climate change on global water resources *Glob. Environ. Change* **21** 592–603

Arnell N W *et al* 2013 A global assessment of the effects of climate policy on the impacts of climate change *Nature Clim. Change* **3** 512–9

Bates B C, Kundzewicz Z W, Wu S and Palutikof J P (ed) 2008 *Climate Change and Water. IPCC Technical Paper VI* (Geneva: IPCC)

Bondeau A *et al* 2007 Modelling the role of agriculture for the 20th century global terrestrial carbon balance *Glob. Change Biol.* **13** 679–706

Diffenbaugh N S and Field C B 2013 Changes in ecologically critical terrestrial climate conditions *Science* **341** 486–92

Fader M, Gerten D, Thammer M, Heinke J, Lotze-Campen H, Lucht W and Cramer W 2011 Internal and external green-blue agricultural water footprints of nations, and related water and land savings through trade *Hydrol. Earth Syst. Sci.* **15** 1641–60

Fader M, Rost S, Müller C, Bondeau A and Gerten D 2010 Virtual water content of temperate cereals and maize: present and potential future patterns *J. Hydrol.* **384** 218–31

Falkenmark M and Widstrand C 1992 Population and water resources: a delicate balance *Popul. Bull.* **47** 1–36

Fung F, Lopez A and New M 2010 Water availability in +2 °C and +4 °C worlds *Phil. Trans. R. Soc.* A **369** 99–116

Füssel H-M 2010 How inequitable is the global distribution of responsibility, capability, and vulnerability to climate change: a comprehensive indicator-based assessment *Glob. Environ. Change* **20** 597–611

Gerber S, Joos F and Prentice I C 2004 Sensitivity of a dynamic global vegetation model to climate and atmospheric CO_2 *Glob. Change Biol.* **10** 1223–39

Gerten D, Heinke J, Hoff H, Biemans H, Fader M and Waha K 2011 Global water availability and requirements for future food production *J. Hydrometeorol.* **12** 885–99

Gerten D, Schaphoff S, Haberlandt U, Lucht W and Sitch S 2004 Terrestrial vegetation and water balance: hydrological evaluation of a dynamic global vegetation model *J. Hydrol.* **286** 249–70

Gosling S N, Bretherton D, Haines K and Arnell N W 2010 Global hydrology modelling and uncertainty: running multiple ensembles with a campus grid *Phil. Trans. R. Soc.* A **368** 4005–21

Grübler A, O'Neill B, Riahi K, Chirkov V, Goujon A, Kolp P, Prommer I, Scherbov S and Slentoe E 2007 Regional, national, and spatially explicit scenarios of demographic and economic change based on SRES *Technol. Forecast. Soc. Change* **74** 980–1029

Haddeland I *et al* 2011 Multi-model estimate of the global water balance: setup and first results *J. Hydrometeorol.* **12** 869–84

Hare W L, Cramer W, Schaeffer M, Battaglini A and Jaeger C C 2011 Climate hotspots: key vulnerable regions, climate change and limits to warming *Reg. Environ. Change* **11** S1–13

Hawkins E and Sutton R 2010 The potential to narrow uncertainty in projections of regional precipitation change *Clim. Dyn.* **37** 407–18

Heinke J, Ostberg S, Schaphoff S, Frieler K, Müller C, Gerten D, Meinshausen M and Lucht W 2012 A new dataset for systematic assessments of climate change impacts as a function of global warming *Geosci. Model. Dev. Discuss.* **5** 3533–72

Heyder U, Schaphoff S, Gerten D and Lucht W 2011 Risk of severe climate change impact on the terrestrial biosphere *Environ. Res. Lett.* **6** 034036

Hickler T, Prentice I C, Smith B, Sykes M T and Zaehle S 2006 Implementing plant hydraulic architecture within the LPJ dynamic global vegetation model *Glob. Ecol. Biogeogr.* **15** 567–77

Higgins S I and Scheiter S 2012 Atmospheric CO_2 forces abrupt vegetation shifts locally, but not globally *Nature* **488** 209–12

Huntingford C *et al* 2013 Simulated resilience of tropical rainforests to CO_2-induced climate change *Nature Geosci.* **6** 268–73

Joshi M, Hawkins E, Sutton R, Lowe J and Frame D 2011 Projections of when temperature change will exceed 2 °C above pre-industrial levels *Nature Clim. Change* **1** 407–12

Kier G, Kreft H, Ming Lee T, Jetz W, Ibisch P L, Nowicki C, Mutke J and Barthlott W 2009 A global assessment of endemism and species richness across island and mainland regions *Proc. Natl Acad. Sci. USA* **106** 9322–7

Knopf B, Kowarsch M, Flachsland C and Edenhofer O 2012 The 2 °C target reconsidered *Climate Change, Justice and Sustainability: Linking Climate and Development Policy* ed O Edenhofer (Berlin: Springer) pp 121–38

Knutti R, Furrer R, Tebaldi C, Cermak J and Meehl G A 2010 Challenges in combining projections from multiple climate models *J. Clim.* **23** 2739–58

Knutti R and Sedláček J 2012 Robustness and uncertainties in the new CMIP5 climate model projections *Nature Clim. Change* **3** 369–73

Kundzewicz Z W, Mata L J, Arnell N W, Döll P, Jimenez B, Miller K, Oki T, Şen Z and Shiklomanov I 2008 The implications of projected climate change for freshwater resources and their management *Hydrol. Sci. J.* **53** 3–10

Leemans R and Eickhout B 2004 Another reason for concern: regional and global impacts on ecosystems for different levels of climate change *Glob. Environ. Change* **14** 219–28

Lehner B, Döll P, Alcamo J, Henrichs T and Kaspar F 2006 Estimating the impact of global change on flood and drought risks in Europe: a continental, integrated analysis *Clim. Change* **75** 273–99
Leipprand A and Gerten D 2006 Global effects of doubled atmospheric CO_2 content on evapotranspiration, soil moisture, and runoff *Hydrol. Sci. J.* **51** 171–85
Lenton T M 2011 Beyond 2 °C: redefining dangerous climate change for physical systems *WIREs Clim. Change* **2** 451–61
Lenton T M, Held H, Kriegler E, Hall J W, Lucht W, Rahmstorf S and Schellnhuber H J 2008 Tipping elements in the earth's climate system *Proc. Natl Acad. Sci. USA* **105** 1786–93
Levermann A *et al* 2012 Potential climatic transitions with profound impact on Europe—review of the current state of six 'tipping elements of the climate system' *Clim. Change* **110** 845–78
Li F, Zeng X D and Levis S 2012 A process-based fire parameterization of intermediate complexity in a dynamic global vegetation model *Biogeosciences* **9** 2761–80
Loarie S R, Duffy P B, Hamilton H, Asner G P, Field C B and Ackerly D D 2009 The velocity of climate change *Nature* **462** 1052–5
Lucht W, Prentice I C, Myneni R B, Sitch S, Friedlingstein P, Cramer W, Bousquet P, Buermann W and Smith B 2002 Climatic control of the high-latitude vegetation greening trend and Pinatubo effect *Science* **296** 1687–9
Mahlstein I, Daniel J S and Solomon S 2013 Pace of shifts in climate regions increases with global temperature *Nature Clim. Change* **3** 739–43
Mahlstein I, Knutti R, Solomon S and Portmann R W 2011 Early onset of significant local warming in low latitude countries *Environ. Res. Lett.* **6** 034009
Masson D and Knutti R 2011 Climate model genealogy *Geophys. Res. Lett.* **38** L08703
Mastrandrea M D *et al* 2010 *Guidance Note for Lead Authors of the IPCC 5th Assessment Report on Consistent Treatment of Uncertainties* (Geneva: IPCC)
Meehl G A, Covey C, Delworth T, Latif M, McAvaney B, Mitchell J F B, Stouffer R J and Taylor K E 2007 The WCRP CMIP3 multimodel dataset: a new era in climate change research *Bull. Am. Meteorol. Soc.* **88** 1383–94
Meinshausen M, Raper S C B and Wigley T M L 2011 Emulating coupled atmosphere–ocean and carbon cycle models with a simpler model, MAGICC6—part 1: model description and calibration *Atmos. Chem. Phys.* **11** 1417–56
Millar C I, Stephenson N L and Stephens S L 2007 Climate change and forests of the future: managing in the face of uncertainty *Ecol. Appl.* **17** 2145–51
Milly P C D, Betancourt J, Falkenmark M, Hirsch R M, Kundzewicz Z W, Lettenmaier D P and Stouffer R J 2008 Stationarity is dead: whither water management? *Science* **319** 573–4
Mitchell T D 2003 Pattern scaling: an examination of the accuracy of the technique for describing future climates *Clim. Change* **60** 217–42
Mitchell T D and Jones P D 2005 An improved method of constructing a database of monthly climate observations and associated high-resolution grids *Int. J. Climatol.* **25** 693–712
Murray S J, Watson I M and Prentice I C 2013 The use of dynamic global vegetation models for simulating hydrology and the potential integration of satellite observations *Prog. Phys. Geogr.* **36** 63–97
Ostberg S, Lucht W, Schaphoff S and Gerten D 2013 Critical impacts of global warming on land ecosystems *Earth Syst. Dyn. Discuss.* **4** 541–65
Parry M, Arnell N, McMichael T, Nicholls R, Martens P, Kovats S, Livermore M, Rosenzweig C, Iglesias A and Fischer G 2001 Millions at risk: defining critical climate change threats and targets *Glob. Environ. Change* **11** 181–3
Pennell C and Reichler T 2011 On the effective number of climate models *J. Clim.* **24** 2358–67
Piao S *et al* 2013 Evaluation of terrestrial carbon cycle models for their response to climate variability and to CO_2 trends *Glob. Change Biol.* **19** 2117–32
Pincus R, Batstone C P, Hofamnn R J P, Taylor K E and Glecker P J 2008 Evaluating the present-day simulation of clouds, precipitation, and radiation in climate models *J. Geophys. Res.* **113** 1–10
Piontek F *et al* 2013 Leaving the world as we know it: hotspots of global climate change impacts *Proc. Natl Acad. Sci. USA* at press
Rammig A, Jupp T E, Thonicke K, Tietjen B, Heinke J, Ostberg S, Lucht W, Cramer W and Cox P M 2010 Estimating the risk of Amazonian forest dieback *New Phytol.* **187** 694–706
Rogelj J, Meinshausen M and Knutti R 2012 Global warming under old and new scenarios using IPCC climate sensitivity range estimates *Nature Clim. Change* **2** 248–53
Rogelj J, Nabel J, Chen C, Hare W, Markmann K, Meinshausen M, Schaeffer M, Macey K and Höhne N 2010 Copenhagen accord pledges are paltry *Nature* **464** 1126–8
Rost S, Gerten D, Bondeau A, Lucht W, Rohwer J and Schaphoff S 2008 Agricultural green and blue water consumption and its influence on the global water system *Water Resour. Res.* **44** W09405
Rost S, Gerten D, Hoff H, Lucht W, Falkenmark M and Rockström J 2009 Global potential to increase crop production through water management in rainfed agriculture *Environ. Res. Lett.* **4** 044002
Rowlands D J *et al* 2012 Broad range of 2050 warming from an observationally constrained large climate model ensemble *Nature Geosci.* **5** 256–60
Rudolf B, Becker A, Schneider U, Meyer-Christoffer A and Ziese M 2010 *GPCC: Status Report December 2010 on the Most Recent Gridded Global Data Set Issued in Fall 2010 by the Global Precipitation Climatology Centre* (Offenbach: DWD/GPCC)
Sandel B, Arge L, Dalsgaard B, Davies R G, Gaston K J, Sutherland W J and Svenning J C 2011 The influence of late quaternary climate-change velocity on species endemism *Science* **334** 660–4
Schaphoff S, Heyder U, Ostberg S, Gerten D, Heinke J and Lucht W 2013 Contribution of permafrost soils to the global carbon budget *Environ. Res. Lett.* **8** 014026
Schellnhuber J, Warren R, Haxeltine A and Naylor L 2004 Integrated assessment of benefits of climate policy *OECD, The Benefits of Climate Change Policies* (Paris: OECD) pp 83–110
Schewe J *et al* 2013 Multi-model assessment of water scarcity under climate change *Proc. Natl Acad. Sci. USA* at press
Schneider S H and Mastrandrea M D 2005 Probabilistic assessment of dangerous climate change and emissions pathways *Proc. Natl Acad. Sci. USA* **102** 15728–35
Schneider von Deimling T, Meinshausen M, Levermann A, Huber V, Frieler K, Lawrence D M and Brovkin V 2012 Estimating the near-surface permafrost-carbon feedback on global warming *Biogeosciences* **9** 649–65
Scholze M, Knorr W, Arnell N W and Prentice I C 2006 A climate-change risk analysis for world ecosystems *Proc. Natl Acad. Sci. USA* **103** 13116–20
Sitch S *et al* 2003 Evaluation of ecosystem dynamics, plant geography and terrestrial carbon cycling in the LPJ dynamic global vegetation model *Glob. Change Biol.* **9** 161–85
Sitch S *et al* 2008 Evaluation of the terrestrial carbon cycle, future plant geography and climate–carbon cycle feedbacks using five dynamic global vegetation models (DGVMs) *Glob. Change Biol.* **14** 2015–39
Smith J B *et al* 2009 Assessing dangerous climate change through an update of the Intergovernmental Panel on Climate Change (IPCC) reasons for concern *Proc. Natl Acad. Sci. USA* **106** 4133–7
Sommer J H, Kreft H, Kier G, Jetz W, Mutke J and Barthlott W 2010 Projected impacts of climate change on regional capacities for global plant species richness *Proc. R. Soc.* B **277** 2271–80

Srinivasan U T, Carey S P, Hallstein E, Higgins P A T, Kerr A C, Koteen L E, Smith A B, Watson R, Harte J and Norgaard R B 2008 The debt of nations and the distribution of ecological impacts from human activities *Proc. Natl Acad. Sci. USA* **105** 1768–73

Sykes M T, Prentice I C and Laarif F 1999 Quantifying the impact of global climate change on potential natural vegetation *Clim. Change* **41** 37–52

Tang Q and Lettenmaier D P 2012 21st century runoff sensitivities of major global river basins *Geophys. Res. Lett.* **39** L06403

Thonicke K, Venevsky S, Sitch S and Cramer W 2001 The role of fire disturbance for global vegetation dynamics: coupling fire into a dynamic global vegetation model *Glob. Ecol. Biogeogr.* **10** 661–77

UNFCCC 2011 *UNFCCC Report of the Conf. of the Parties on its Sixteenth Session, Held in Cancún from 29 November to 10 December 2010* (http://unfccc.int/resource/docs/2010/cop16/eng/07a01.pdf)

Warren R, Price J, Fischlin A, de la Nava Santos S and Midgley G 2011 Increasing impacts of climate change upon ecosystems with increasing global mean temperature rise *Clim. Change* **106** 141–77

Zelazowski P, Malhi Y, Huntingford C, Sitch S and Fisher J B 2011 Changes in the potential distribution of humid tropical forests on a warmer planet *Phil. Trans. R. Soc.* A **369** 137–60